

Enhanced Dielectric-Barrier-Discharge Body-Force Generation Using Nanofoam Materials with Infused Catalytic Layer

Project WBS Number: 694478.052.93.02.11.19.23

Investigator(s): Emilie J. Siochi and Stephen P. Wilkinson (NASA LaRC), Godfrey Sauti and Tian-Bing Xu (NIA)

Purpose

The purpose of this Phase I study was to begin a cross-disciplinary investigation of the link between chemical composition and chemical structure of dielectric materials and DBD actuator body force generation, drawing on NASA and NIA expertise in materials, fluid mechanics and plasmas.

Background

Dielectric-Barrier-Discharge (DBD) actuators are surface-mounted, weakly ionized gas (or plasma) devices consisting of pairs of electrodes separated by a dielectric and operated at high AC voltages. A typical arrangement is shown in Figure 1. The electrically charged dielectric surface attracts ions in the air plasma, imparting momentum to the non-ionized air through many molecular collisions resulting in an effective continuum body force. The body force causes an approximately two-dimensional, zero-net-mass-flux wall jet at the surface that can be used in a number of flow control applications, most notably boundary layer separation control. Recent reviews describing the DBD actuator, its physics and potential uses can found in References [1] and [2].

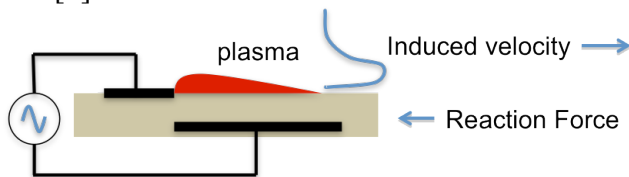


Figure 1: DBD Schematic

While DBD's have been shown to be useful in a number of laboratory flow control demonstrations, they have yet to be widely deployed in aeronautical systems. Reasons for this implementation delay include the need to identify beneficial applications and requirements, a general preference for fully passive devices, and a perception that DBDs are weak flow control

devices. Using a performance metric now used extensively throughout the DBD research community, the reaction force per spanwise unit of actuator length, the state-of-the-art is several hundred milli-Newtons per meter for thick dielectrics operated at very high voltages. Older DBD technology using thin polymer dielectrics (e.g., Kapton) generated an order of magnitude less force and demonstrated flow control in wind tunnel tests at wing chord Reynolds numbers up to 1.2×10^6 . The newer, thick dielectric technology with higher forces should produce higher Reynolds number results placing DBD technology in the range of useful, low speed flight applications.

Optimization of the DBD actuator reported in 2009 by researchers at the University of Notre Dame [3] described effects of dielectric material and thickness, applied voltage amplitude and frequency, voltage waveforms, exposed electrode geometry, covered electrode width, and multiple actuators arrays. It was determined that thick dielectrics with low permittivity operated at low frequencies delivered the highest body force before saturation occurred. Beyond the saturation point, further increase in applied voltage did not significantly increase body force. This effect was attributed to formation of plasma streamers, the number of which vary directly with the applied voltage above the saturation voltage.

Materials investigations were also carried out at the University of Florida in conjunction with the DARPA WEAV (Wingless Electromagnetic Air Vehicle) Phase 1 Seedling award. One of the materials investigated was lightweight silica aerogel (a nanofoam material) although the data has not been made publically available. Related data for the silica aerogel under UF/AFOSR funding is, however, available [4]. The main finding of that study was that aerogel shows a

higher force saturation threshold than conventional dielectric materials and has superior body-force-to-weight ratio, making it well suited for micro air vehicle applications. A difficulty the aerogels have, however, is their extreme fragility.

This report builds on the DBD materials studies of Notre Dame and the University of Florida by establishing a cross-disciplinary team with expertise in fundamental material sciences, fluid mechanics and plasmas. Prior to this Seedling, it was observed that DBD investigations reported in the literature used commercially available dielectric materials such as Kapton, Teflon, Plexiglass and glass, rather than materials specifically designed and engineered for DBD use. While the most relevant material property for DBD work is clearly the breakdown voltage, other parameters including permittivity, loss tangent, plasma erosion/corrosion effects, long term endurance, internal void “partial” discharges and, possibly, a range of not-well-defined electrical surface effects that may influence electrical charge boundary conditions, and hence body force production, are all within the scope of a cross-disciplinary DBD material investigation. Such an effort affords the dual purpose of developing materials based on the current understanding of DBD plasma physics and providing testing opportunities for new material findings that may advance DBD performance and/or understanding of its physics.

Approach

In the Phase I study, we proposed an experimental study of nanofoams and aerogels, with and without an infused catalytic layer to enhance the body-force-generating ability, with the objective of quantifying the performance of various nanofoam dielectric materials and catalytic coatings. This effort was postponed due to the extreme fragility of the initial silica aerogel material and the need to design workable models for force testing. More robust aerogel materials designed and synthesized in collaboration with Glenn Research Center will greatly accelerate our materials development effort.

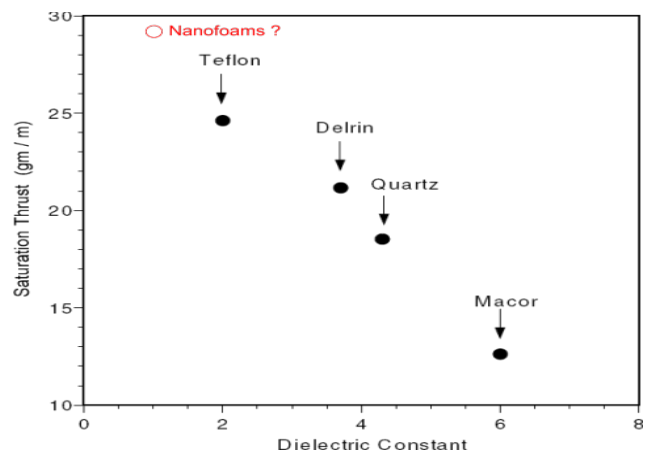


Figure 2. Proposed approach of nanofoams for enhanced saturation force. Adapted from [3].

The revised approach for Phase 1 was to survey commonly used dielectric materials and experimentally characterize both their electrical and body force production properties. Analysis of material behavior differences with respect to material composition, plasma generation and influence on fluid mechanics provided insight on the role of materials design on actuator performance. Based on reference 3 results, increased body force generation is associated with a dielectric constant near unity (currently 2-4), a high breakdown strength (many kV/mm) and low dielectric loss to reduce heat generation. Reference 5 shows that a catalytic coating of titanium oxide can increase body force production by 30%. An investigation of catalytic materials is therefore part of the current studies.

Summary of Research

Materials Selection

Materials included in the test matrix for Phase I are shown in Table 1, along with their chemical structures. The materials tested were in the form of sheets and foams. The structures span the range of inorganic, amorphous glass, alkyl containing acrylic, structural polymers with varying contents of aromatic groups and Teflon, which is a fluorocarbon. The range of materials selected covers readily available commercial polymers such as acrylic (PMMA) and polycarbonate (Lexan), materials widely used in the DBD literature including, Kapton, glass and Teflon, as well as high performance, aerospace grade materials such as PEEK and Upilex. These

materials were characterized to determine their dielectric constants and dielectric strengths. Following those measurements, DBD models were constructed and characterized to determine the body force generated.

Table 1. List of materials studied

Trade (Common) Name	Chemical Name/Class	Unit Formula	Form
Glass	Silica	SiO ₂ + Na ₂ O + CaO	Sheet, Nanofoam (Aerogel)
Teflon (PTFE)	Polyterafuoroethylene	C ₂ F ₄	Sheet
PMMA (Acrylic)	Polymethylmethacrylate	C ₅ O ₂ H ₈	Sheet
Lexan	Polycarbonate	C ₁₆ H ₁₀ O ₃	Sheet
ULTEM	Polyetherimide	C ₁₇ H ₁₂ O ₃ N ₂	Sheet, Foam
PEEK	Polyetheretherketone	C ₂₁ H ₁₈ O ₃	Sheet
Kapton	Polyimide	C ₁₃ H ₁₀ N ₂ O ₅	Thin* Sheet
Upilex	Polyimide	C ₁₈ H ₁₂ N ₂ O ₄	Thin Sheet, Foam
Solimide	Polyimide	-	Foam (3 densities)
Performa H	Polyimide	-	Foam
Thermalux	Polysulfone	C ₇ H ₈ O ₂ S	Thin Sheet
Boron Nitride (hBN)	Ceramic	BN	Sheet, Spray
PZT	Ceramic	Pb(Zr,Ti _{1-x})O ₃ 0.5x<1	Disk

* t < 1 mm

Dielectric Materials Characterization

The dielectric breakdown strength and the complex dielectric constant are two dielectric properties of particular significance to the performance of DBD actuators. It has also been shown that the capacitance of the test actuator (and hence dielectric constant for a fixed geometry) affects the saturation or maximum thrust that can be generated by increasing the voltage [3]. High dielectric losses lead to heating of the dielectric and thus a decrease in efficiency. These properties are related to the chemistry and microstructure of the dielectric. To determine the dielectric constant and loss as a function of frequency, a Novocontrol Broadband Dielectric Spectrometer and Solartron 1260 Impedance Gain/Phase Analyzer combination was used for measurements in the frequency range 10⁻² Hz to 10⁶ Hz at 30 °C and 120 °C. The samples were placed in a BDS 1200 standard sample cell and temperature was controlled by the Novotherm control system (range 20 °C to 400 °C). Additional installed capacity (Novocool system) covers temperatures down to -100 °C. The test instruments were controlled by commercial WinDETA test software. The extended (beyond actuator test) frequency and temperature range provide for greater insight into the chemical properties of the material that may have a bearing

on actuator performance. Additional measurements for the very low dielectric constant materials were conducted in a custom-built sample cell with smaller stray capacitance contributions to the measurement. These measurements were conducted at room temperature and used as a basis for stray capacitance corrections to the BDS cell data.

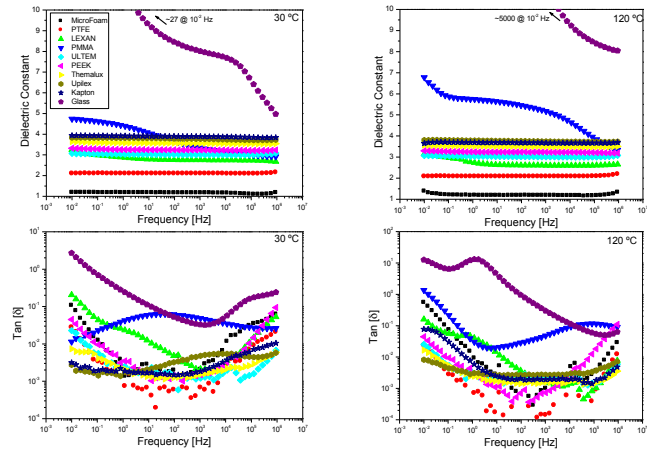


Figure 3. Dielectric constants and loss tangents of the materials studied

Table 2: Dielectric constant and Tan δ at 5 kHz, the actuators’ test frequency.

Material	ε	Tan δ (x 10 ⁻⁴)
PZT	1851	161
Glass	7.8	39.1
Kapton	3.9	2.8
Upilex	3.8	5.4
Thermalux	3.6	1.9
PEEK	3.2	2.2
ULTEM	3.0	1.3
PMMA	3.2	38.7
Lexan	2.7	2.5
Teflon	2.1	0.9
Micro Foam	1.2	4.8
Boron Nitride	4*	4.0

* Measurement pending. Value from literature.

All the dielectric measurements were small signal measurements with an excitation voltage in the order of 1 V. It was assumed that the dielectric properties do not change significantly at the high (kV) voltages at which the actuators are tested, an assumption that is going further investigated.

Figure 3 shows the dielectric constant and loss tangent ($\tan \delta$) of the various materials tested. Apart from PZT ($\epsilon > 1000$) which is not included in the plots, glass has the highest dielectric constant with a highly frequency and temperature dependent value that is greater than 5.5. This is to be expected for glasses that in addition to SiO_2 , contain a range of ions, whose mobility is both frequency and temperature dependent. The polymeric materials have dielectric constants in the range 2 to 5 and with the exception of PMMA, these are largely frequency independent. The foam has the lowest ϵ with frequency independent values just above one. The polymers and foam have low losses with $\tan \delta$ ranging from 10^{-2} to 10^{-1} . $\tan \delta$ rises to 10 for the glass. The dielectric constant and $\tan \delta$ data at 30 °C and the actuator test frequency (5 kHz) are summarized in Table 2.

The dielectric breakdown strength of a material is important in determining whether or not a sufficient voltage can be sustained to enable the formation of a plasma. For porous dielectrics, two breakdown regimes are of importance, one in which the material completely fails and therefore cannot be tested any further and a second one where there is no breakdown through the entire specimen but partial discharges occur within the pores. It was a major assumption in this work that as the pore sizes in foamy dielectrics decreased, the initial decrease in the overall breakdown voltage would be replaced first by breakdown being limited to the pores in micro foams (with no plasma appearing on the surface), to plasma generation with nano-porous dielectrics. For enhanced actuation, this change in breakdown characteristics must occur with the ultra-low dielectric constants that arise from the porous structure being maintained.

The dielectric breakdown in porous dielectrics and its relation to plasma formation is illustrated in Figure 4. With large pores, there is complete breakdown of the specimen while partial discharges occur in the micro sized pores both of

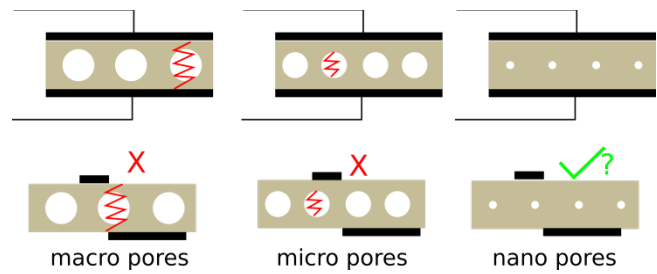


Figure 4: Diagram of dielectric breakdown in porous dielectrics and its relation to plasma formation.

which prevent plasma formation. Hrubesh [8] described how in nanoporous media, such as silica aerogels, the pore size becomes so small that it prevents dielectric breakdown as the necessary electron acceleration processes are inhibited leading to plasma formation [3].

To screen the breakdown characteristics of candidate actuator materials, a dielectric breakdown test setup consisting of a set of a 51 mm diameter opposing cylinders ASTM standard electrodes (Hipotronics TF-2-50), a 10 kV high voltage amplifier (Trek 10/10B), signal generator (Philips PM5138A), as well as ac voltage and current monitors (Keithley 2000 and Keithley 2100) was assembled. The sample stage was placed in a custom built Plexiglas box, both to shield the test specimens as well as for operator safety. Schematic of the test set-up is shown in Figure 5. All the dielectric breakdown tests were conducted in air in accordance with ASTM D149, Test Method for Dielectric Breakdown Voltage and Dielectric Strength of Solid Electrical Insulating Materials at Commercial Power Frequencies [9].

The instruments for this test were all controlled by custom design dBt software that was written as a part of this project. Among the features of this software are the ability to set up different tests (voltage rates, steps) to match various ASTM standards as well as custom test profiles, a number of ways of specifying the termination criterion, real-time monitoring of the applied voltage and leakage current through the dielectric and the ability to graph all this data in various 2D and 3D views. The leakage current data is useful

where the material might not breakdown but still pass so much current that it affects the actuator performance. The software also features an integrated user management layer, including logbook that, in multi-user environments, would be required to monitor the safe use of such high voltage equipment.

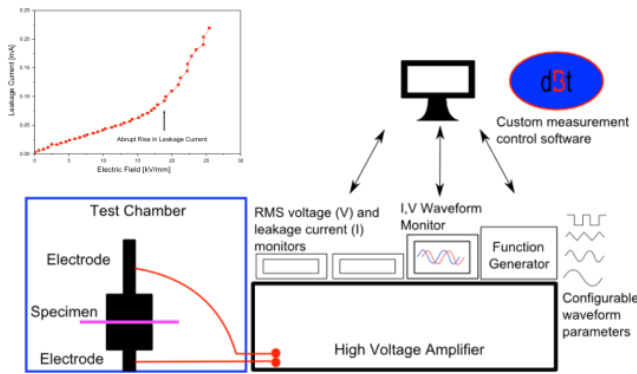


Figure 5. Schematic of the equipment setup developed for dielectric breakdown strength testing under the seedling funding.

With the exception of commercial foams with as received thicknesses less than 2 mm, all test materials passed the 10 kV dielectric breakdown screening tests with maximum leakage currents less than 5 mA.

Accomplishments

The apparatus for performing the dielectric and force measurements had to be constructed in Phase I. The accomplishments for this Seedling activity thus include the establishment of in-house characterization capabilities for the design and evaluation of enhanced DBD actuators at LaRC. This is a valuable resource not only for NASA, but also for the DBD community for which lack of good dielectric characterization of materials is a deficiency in the development of plasma actuators.

DBD Actuator Performance

Force Measurements

The DBD force measurement apparatus is shown schematically in Figure 6. The system is centered around an analytical mass balance (Sartorius Model CPA 324S). The balance was housed in a 12 ft³ Plexiglass enclosure to shield the balance

from room air drafts, for personnel safety from the high operating voltage in the enclosure, and to collect and vent gas generated by the plasma. The model was mounted on an insulating post away from the balance and connected to the power supply with brass ball chain to minimize parasitic force.

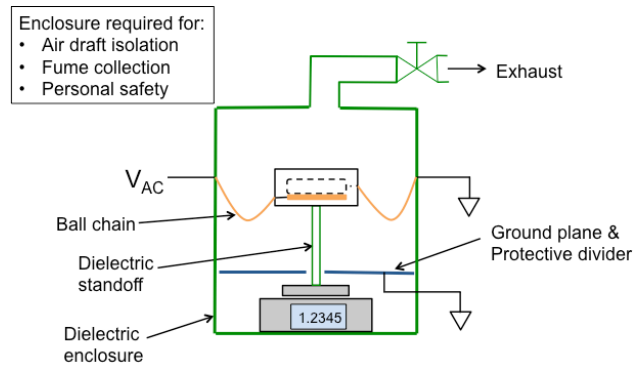


Figure 6. Schematic drawing of DBD thrust measurement apparatus.

Figure 7 shows the notation used for DBD model dimensions and corresponding values are shown in Table 3.

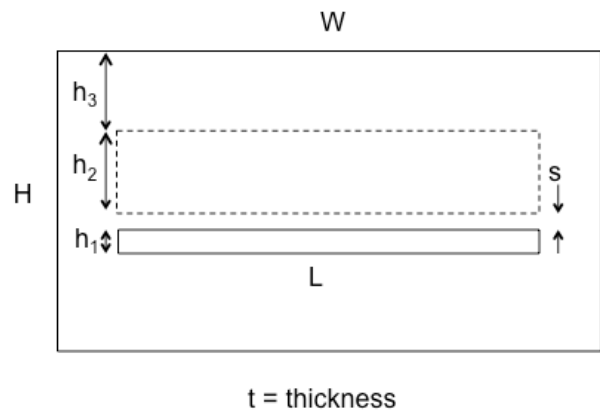


Figure 7. DBD thrust model dimension designations

Table 3. DBD thrust models. See Figure 7 for notation. All dimensions in millimeter.

Model	Material	H	W	t	h1	h2	h3	L	s	Plasma Initiation kVpp / kHz
S108	PMMA	124	197	2	5	15	61	150	0	6.3/5
S109	LEXAN	120	203	2.3	5	15	60	150	0	6.6/5
S110	ULTEM	120	153	3.2	5	15	60	124	0	6.9/5
S111	PEEK	116	153	3.1	5	15	58	120	0	7.6/5
S113	GLASS	104	153	1.2	5	15	57	120	0	5.6/5
S114	PFTE	120	153	3.3	5	15	60	113	0	8.6/5
S118	Boron Nitride	102	152	7.3	5	15	50	120	0	7.3/5

The thrust for the models listed in Table 3 was measured on the thrust apparatus. A critical parameter was the plasma initiation voltage listed in the last column of Table 3. They correspond to the first appearance of current spikes characteristic of plasma breakdown.

Figure 8 shows a photograph of a glass model. The plasma in this case has not reached saturation as evidenced by the lack of plasma streamers. Note also that the plasma is well within the area of the covered electrode.

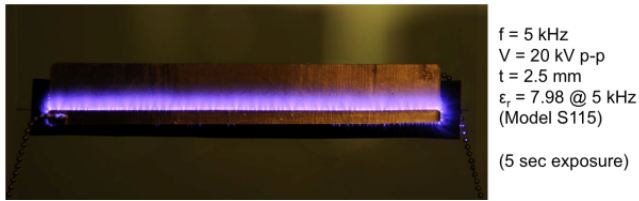


Figure 8. Glass DBD Actuator in operation.

In order to assess the sensitivity of the DBD thrust generation to different dielectric materials, all other thrust sensitivities must either be known, computed or held constant as the materials are varied. A significant difficulty lies in the frequency dependency of the DBD actuator, both plasma and electrical. In the plasma case, mean thrust is generated as the time average of many, rapid, small impulses occurring twice per excitation cycle [2]. Increasing activation frequency contributes directly to increased thrust. In the electrical case, the DBD actuator is an electrical circuit element with both passive capacitive properties (geometry and dielectric permittivity) and active plasma characteristics (gaseous ionization/recombination events, time-varying plasma resistance and capacitance). The electrical frequency response stems from both. One of the challenges for follow-on phase 2 work is to account for such frequency effects in order to assess underlying differences among materials that may affect their thrust generation capability.

In this Phase 1 investigation, as much was held constant as possible such as a common model geometry, electrode pattern, power supply, waveform, wiring and diagnostics. The remaining variables were dielectric thickness and coefficient, excitation voltage and frequency. A

fixed frequency of 5 kHz was chosen for these preliminary studies. With these four parameters, a scaling method is required to compare different models.

Voltage Normalization

A preliminary attempt was made to normalize data to approximately account for known thrust sensitivities. Such an approach was developed by Orlov et al. [7] with a lumped parameter equivalent circuit of the actuator and plasma. This method can account for the impact of dominant parameters including thickness, dielectric constant, voltage and frequency. The method, however, requires numerical computation of the time-dependent charge distribution in order to provide boundary conditions for the electric field equation used to calculate actuator body force. Such effort was beyond the scope of the current investigation and an alternative simplified approach was used. The simplified approach is to examine a one-dimensional DBD actuator from which an assessment of the main electrical properties of the 2D case can be obtained. It cannot deal with 2D electric field distribution effects believed to be the mechanism by which thick dielectrics achieve higher body force [3].

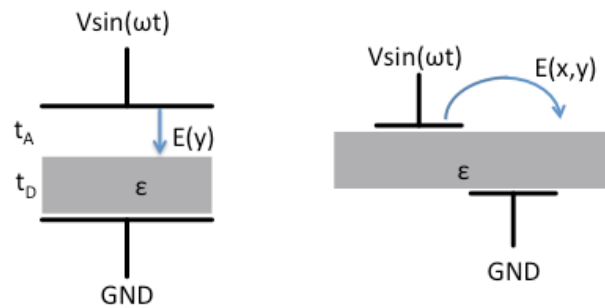


Figure 9. (a) One dimensional DBD actuator (partially filled capacitor), (b) standard two-dimensional (or asymmetric) DBD actuator. $E(y)$ and $E(x,y)$ denote 1D and 2D electric fields.

The one-dimensional version of a DBD actuator is partially filled capacitor (neglecting edge fringe effects) as illustrated in Figure 9(a) in comparison to the 2D asymmetric DBD actuator in Figure 9(b). Whereas the air gap in which plasma breakdown occurs in the 1D case is characterized

by a single dimension (t_A), the gap in the 2D case is represented by an electric field distribution region, $E(x,y)$ that is presumed to be computable given the charge boundary conditions.

For the 1D case, simple relations among the electric fields, dielectric coefficients, voltages and dimensions are easily obtained. Using the fact that the electric displacement (D) field remains constant across the air and dielectric in Figure 9(a), a simple expression relating the applied voltage, air gap electric field, dielectric permittivities and dimensions can be obtained:

$$V = E_a \left(t_a + \frac{t_d}{\epsilon_d} \right) \quad (1)$$

Equation 1 shows that the voltage across the 1D actuator is equal to the electric field in the air gap, E_a , modified by a term comprised of the thicknesses and permittivity of the air and dielectric material. From Paschen’s law for plasma breakdown, the breakdown voltage is a unique function of the pressure-electrode displacement product (Pd) for each gas. At a given pressure, breakdown occurs at unique values of V and d , so the electric field at breakdown is also unique (i.e., $E=V/d$). If E_a is solely a function of pressure the according to the equation 1, V at breakdown implicitly includes the effect of both thicknesses (t_a and t_d) and the dielectric's permittivity (ϵ_d). This suggests that V at initial breakdown is a useful normalization parameter that can be used to account for the electrical performance at a fixed frequency.

DBD Thrust Data

Figure 10 shows the thrust data for the seven materials in Table 2 plotted against the applied voltage normalized by the plasma initiation voltage, V_{init} . The first observation is that all of the force data follow a power law behavior, $Thrust \propto (V/V_{init})^n$, where the exponent is in the range $4.8 < n < 6.1$. This is in the range of values reported by other

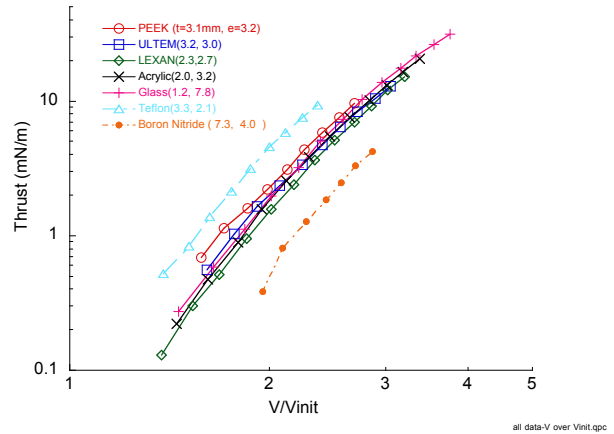


Figure 10. DBD actuator thrust vs. relative voltage. V_{init} is the applied voltage at which plasma first appear. The legend lists the materials along with their thickness and relative dielectric constant from Table 2.

investigators. The reason for the variation among the different materials has not yet been investigated. The second observation is that none of the curves show force saturation. This was an expected result since the maximum voltage from the high voltage amplifier was 20 kV peak-to-peak. Other investigators reporting saturation effects required voltages 3-4 times this level. A step up transformer for the HV amplifier has been procured and is available for Phase 2 studies. A third observation in Figure 10 is the data groupings. The organic hydrocarbons and glass fall in a distinct group with Teflon, a fluorinated polymer, and boron nitride, an inorganic compound at higher and lower level. These groupings are highly dependent upon the nature and validity of the voltage normalization. In phase 2 studies, we will investigate the possibility of links between such behavior and chemical composition and structure.

Of note in the results here is the influence of chemical structure on the thrust generated. As one moves from the right side of the graph in Figure 10 towards the left, dielectric constant is decreasing. The ranking of dielectric constants is therefore glass > acrylic > polycarbonate > Ultem~PEEK > Teflon. Of interest here is the separation of the thrust lines as a function of aromatic content of these materials. Examination

of the chemical structures yields two observations. The first is that greater aromatic content, i.e. more benzene groups in the polymer chain versus alkyl content, contributes to greater thrust. This is demonstrated by the increasing thrust as one goes from amorphous glass, to alkyl acrylic, to polycarbonate, and finally to polyimides, which have the highest density of aromatic rings. Based on this trend, it can be concluded that polarizability of the functional groups contributes to body force generation. In this case, the resonant structures of the aromatic rings yield high electron density and thus greater polarizability to enhance surface charge concentration.

On the other hand, the source of Teflon's efficacy as a DBD plasma actuator is different. It is likely due to fluorine's electronegativity, i.e. the tendency of fluorine to attract electrons to complete its valence band. Electronegativity is inversely proportional to polarizability, however, it can also contribute to enhanced surface charges due to its affinity for electrons from sources in the vicinity of the actuator surface. This property must be reconciled to the normal operation of the DBD plasma in which charge deposition is responsible for the extinction of the plasma twice per excitation cycle. To enhance performance, the polarity and phase of charge deposition must be considered.

Milestones proposed for Phase I

The milestones and deliverables proposed for Phase I are shown in the Table 4.

Accomplishments not listed in the milestones above include the design and construction of apparatus to accurately measure the dielectric properties and reaction force of the materials in the test matrix. It was necessary to establish these capabilities in-house. It is anticipated that the ranking of the dielectric constants of the bulk form will be in line with the ranking of the foam form of the same material, therefore the trend for initial assessment of thrust is informative. The thrust measurements were completed for the bulk materials for which dielectric properties were obtained. The literature report on the thrust

Table 4. Milestones/Deliverables

Deliverable	Date
Dielectric properties: dielectric constant, loss and breakdown strength of commercially available and NASA developed foams will be determined. This data is currently not available anywhere and will thus be made available in appropriate literature	4Q, FY 11
The dielectric properties of candidate catalytic materials will be determined.	1Q, FY 12
Test actuators will be fabricated from promising candidate materials.	2Q, FY 12
The performance of these test actuators will be evaluated to determine induced flow and reaction force as a function of dielectric properties. The data will be made available in suitable literature.	3Q, FY 12

generated from silica aerogel confirms our hypothesis that nanoporous, low dielectric constant materials will make effective plasma actuators [4]. Measuring the dielectric constants and reaction force generated from the bulk materials first, thus reduces the steps needed to downselect the candidates of chemical compositions that can be foamed and reduces the complexity of the study as we can decrease the number of compositions for which the foaming procedure has to be developed, to the ones that have greater promise for enhanced force generation. Results from silica aerogel showing significant enhancement in body force generated from the porous form of silica [4] point to the promise of a similar improvement in performance from the nanofoam version of low dielectric constant bulk polymers proposed in Phase II.

Next Steps

Aerogels are nanoporous materials whose microstructure imparts these materials with unusual dielectric and electronic properties. Among such properties of interest in DBD plasma actuator design are the extremely low dielectric constants (approaching 1) and high dielectric strengths [3]. Silica aerogels are the most common form of aerogels. These materials are notoriously brittle and thus not suitable for

NARI Seedling Fund – Final Technical Report

practical actuator applications. Therefore, in Phase I, we embarked on identifying robust aerospace grade materials from which low dielectric constant foams could be made. This work included testing the properties of bulk versions of materials as well as readily available micro sized foams of these bulk materials. We demonstrated that a thick (mm's) dielectric with micron size pores will sustain an electric field high enough to generate a plasma. However none has yet been observed on the surface, possibly due to some ionization within the pores. More work is continuing to further investigate this.

Recently published literature affirmed our Phase I hypothesis that aerogels with nanosized pores and dielectric constants close to 1 can indeed make highly efficient actuators [4]. The threshold pore size to enable a plasma to be observed has not yet been established. Our as yet unfinished work on foams of varying porosity will inform some of this. The balance between pore size and actuator performance is one of interest as it determines how robust the actuators can be. Our work will inform on the next generation of these materials that will be robust and efficient enough for applications.

Current TRL

This activity is basic research and is, therefore, at the TRL 1-2 level.

Applicable NASA Programs/Projects

While DBD actuator technology is still in its nascent stages of development, the outlines of potential applications are becoming clear and materials play a vital role in these visions. The impact of DBD technology on NASA's aeronautical challenges depends upon the ultimate level of flow forcing that can be obtained and the creativity in applying such technology in useful ways. Using the reaction force per unit length of a single, asymmetric DBD element tested in still air as a metric, the current state-of-the-art is about 0.25 Newtons/meter force using thick dielectric materials tested at extremely high voltages. This level of force has been shown to be useful in delaying boundary layer separation on low speed airfoils and has generated interest from

the rotorcraft, gas turbine, wind turbine, and trucking industries as well as interest with regard to noise abatement on large aircraft landing gear [1,2]. All such investigations are in various developmental stages and as these efforts advance, issues of material properties including dielectric constant and breakdown strength, dielectric absorption and heating, surface breakdown and chemical release due to adjacent plasma, catalytic effects, manufacturability and long term survival ratings will all become increasingly more important.

Beyond the demonstrated flow separation capability of the DBD actuator, a major, long acknowledged aeronautical challenge for NASA is to reduce viscous drag on aircraft across the speed ranges from low subsonic to supersonic. While we continue to seek higher performance DBD actuators, by focusing on and exploiting the very low speed of the viscous sublayer in a turbulent boundary layer, current DBD technology may be sufficient to yield drag reduction results if deployed in creative ways. One possible approach is to match the scale of the DBD actuators to the physical spacing of the low-speed streak structure observed in the sublayer of turbulent boundary layers. This spacing scales roughly inversely with free stream speed and can reach very small values in actual flight. Materials that have very high dielectric breakdown strength in thin layers will be an enabling component of such a study.

Publications and Patent Applications

Intellectual property developed in this work has been disclosed in an invention disclosure. LAR-18189-1 Enhanced Dielectric-Barrier-Discharge Body-Force Generation Using Nanofoam Material with Infused Catalytic Layer was assigned on March 23, 2012.

References:

1. Moreau E., "Airflow control by non-thermal plasma actuators", J. Phys D: Appl. Phys., V. 40, N. 3, 2007, pp. 605-636.
2. Corke T.C., Enloe C.L. and Wilkinson S.P., "Dielectric Barrier Discharge Plasma Actuators

for Flow Control", *Ann. Rev. Fluid Mech.* V. 42, 2010, pp: 505–29.

3. Thomas F.O., Corke T.C., Iqbal M., Kozlov A. and Scahtzman D., "Optimization of dielectric barrier discharge actuators for active aerodynamic flow control", *AIAA J.*, v. 47, n. 9, Sept., 2009.

4. Durscher R. and Roy S. , "Aerogel and Ferroelectric Dielectric Materials for Plasma Actuators", *J. Phys. D: Appl. Phys.*, 2012, V. 45, N. 1, Art. 012001, Jan. 11, 2012

5. Fine N., Steven Brickner S.: Plasma catalysis for enhanced-thrust single dielectric barrier discharge plasma actuators, *AIAA Journal*, vol.48 no.12, 2010, pp. 2979-2982.

6. Massines F., Rabehi A., Decomps P., Ben Gadri, R. Segur P., Mayoux C.: Experimental and theoretical study of a glow discharge at atmospheric pressure controlled by dielectric barrier, *Journal of Applied Physics*, v. 83, n. 6, Mar 15, 1998, pp. 2950-2957.

7. Orlov D.M., Corke T.C., Patel M.P., "Electric Circuit Model for Aerodynamic Plasma Actuator", *AIAA Paper 2006-1206*, Jan. 2006.

8. Hrubesh, L. W, "Aerogels for Electronics," presented at Technology 2004 NASA, Washington, D. C., November 6-9, 1994.

9. ASTM D149 - 09 Standard Test Method for Dielectric Breakdown Voltage and Dielectric Strength of Solid Electrical Insulating Materials at Commercial Power Frequencies, *ASTM International*, Nov 2009.